Front. Earth Sci. China 2010, 4(3): 363–373
DOI 10.1007/s11707-010-0023-7

RESEARCH ARTICLE

Analysis and characterization of the synergistic AIRS and MODIS cloud-cleared radiances

Hong ZHANG (✉)[1], Hung-Lung HUANG[1,3], Agnes LIM[1], Robert HOLZ[1], Steve DUTCHER[1], Fred NAGLE[1], Liam GUMLEY[1], Jinnian WANG[2], Runhe SHI[3], Wei GAO[3,4]

1 Cooperative Institute for Meteorological Satellite Studies, Space Science and Engineering Center, University of Wisconsin, Madison, WI 53706-1323, USA
2 Institute of Remote Sensing Applications, Chinese Academy of Sciences, Beijing 100864, China
3 Joint Laboratory for Environmental Remote Sensing and Data Assimilation, East China Normal University, Shanghai 200062, China
4 Natural Resource Ecology Laboratory, Colorado State University, Fort Collins, CO 80523-1062, USA

Abstract The Atmospheric Infrared Sounder (AIRS) and MODerate-Resolution Imaging Spectroradiometer (MODIS) on board NASA Earth Observing System (EOS) Aqua spacecraft measure the upwelling infrared radiance used for numerous remote-sensing- and climate-related applications. AIRS provides high spectral resolution infrared radiances, while MODIS provides collocated high spatial resolution radiances at 16 broad infrared bands. An optimal algorithm for cloud-clearing has been developed for AIRS cloudy soundings at the University of Wisconsin-Madison, where the spatially and spectrally collocated AIRS and MODIS data has been used to analyze the characteristic of this algorithm. An analysis and characterization of the global AIRS cloud-cleared radiances using the bias and the standard deviation between the cloud-cleared and the nearby clear measurements are studied. Scene inhomogeneity for both land- and water-surface types has been estimated to account for the assessed error. Both monthly and seasonal changes of global AIRS/MODIS cloud-clearing performance also have been analyzed.

Keywords cloud-clearing, Atmospheric Infrared Sounder (AIRS), MODerate-Resolution Imaging Spectroradiometer (MODIS)

1 Introduction

The Atmospheric Infrared Sounder (AIRS) and the MODerate-Resolution Imaging Spectroradiometer (MODIS) on the National Aeronautics and Space Administration's Earth Observing System (EOS) Aqua satellite enable improved global monitoring of the distribution of global clear and clouds. AIRS is a high spectral resolution infrared (IR) sounder with 2378 channels ($\nu/\Delta\nu$ = 1200, where ν is the wave number, and $\Delta\nu$ is the full-width half maximum of the channel). AIRS measures radiances are in the IR range 3.74 to 15.4 μm with several spectral gaps due to the placement of the limited detector arrays. The main purpose of AIRS is to estimate the atmospheric vertical temperature and water vapor profiles from the Earth's surface to an altitude of 40 km with an Instantaneous Field of View (IFOV) horizontal spatial sampling of 13.5 km at nadir (Aumann, et al., 2003). Due to its relatively coarse spatial resolution, when compared with MODIS, the probability of an AIRS footprint to be completely clear is usually less than 10% (Huang and Smith, 2004). It has been demonstrated that for any satellite infrared sounders with relatively wide fields of view (IFOV size > 10 km), the probability of entirely cloud-free IFOV is surprisingly low. The direct infrared (IR) only cloudy retrieval and assimilation of IR cloudy radiances are currently difficult, if not impossible. The difficulty lies in the efficient and accurate modeling and treatment of the cloud signal portion of the IR measurements. Some efforts have just begun to model the microphysical complexity of clouds and their radiative effects (Zhang et al., 2006). The parameterization of cloud properties to deliver much needed improvements in speed and accuracy of forward radiative transfer models is still under development. Indirect use of cloud contaminated radiance by way of cloud-clearing has since received great attention, as an interim measure to improve both the spatial and spectral yields of satellite infrared radiances and sounding products. One of the important issues related to cloud

Received November 21, 2009; accepted February 21, 2010

E-mail: hong.zhang@ssec.wisc.edu

clearing is how to effectively perform cloud clearing (CC) for the AIRS cloudy footprints, while still retaining its sounding gradient information for various local weather and numerical weather prediction (NWP) applications that require high spatial resolution. Smith et al. (2004) combine Moderate Resolution Imaging Spectroradiometer (MODIS) IR clear radiances and AIRS cloudy for CC using the traditional single band N^* approach. In our study, the multiband CC method developed by Li et al. (2005a) is adopted to retrieve the AIRS clear column radiances by combing the multiband MODIS IR clear radiance observations and the AIRS cloudy radiances on a two-single footprint basis.

In this paper, an AIRS and MODIS collocated global data set has been used to systematically analyze the monthly and seasonal characteristics of the synergistic cloud-cleared radiances over day and night and over homogeneous ocean and inhomogeneous land surfaces. Both bias and Root Mean Square (RMS) error for daily, monthly, and seasonal time periods are examined to further confirm and refine the findings reported in this paper.

2 Overview of synergistic multiband cloud clearing methodology

2.1 Collocation between AIRS and MODIS

AIRS spatial coverage is provided by the scan head assembly, which contains a cross-track rotary scan mirror and calibrators. The AIRS spatial distribution is used in the collocation between the MODIS and AIRS measurement, which is the first step for the multiband MODIS/AIRS cloud clearing. The MODIS pixels with 1-km spatial resolution are collocated within an AIRS footprint (Zhang et al., 2007). With a set of AIRS earth-located observations, the footprint of each AIRS observation describes a shape that is circular at nadir, quasi-ellipsoidal at intermediate scan angles, and ovular at extreme scan angles. The diameter of the AIRS footprint at nadir is approximately 13.5 km. Depending on the angular difference between the AIRS and MODIS slant range vector, a weight (ω) is assigned to each MODIS pixel collocated to AIRS. For example, 100% if the MODIS pixel lies at the center of the AIRS oval, and 0 if at the outer edge. The collocation is modeled efficiently, and the algorithm provides accuracy better than 1 km, assuming the geometrical information from both instruments is accurately known.

2.2 AIRS cloud masking using MODIS

Once the MODIS pixels are collocated with the AIRS IFOV, the cloud properties within the AIRS pixel can be characterized using the MODIS cloud mask (Ackerman et al., 1998). The cloud mask, cloud phase mask, as well as the cloud-layer information mask can be generated from MODIS products with 1-km spatial resolution (Li et al., 2004). For each AIRS IFOV, a clear coverage (0–100%) is created by accounting for the percentage of MODIS pixels designated "confident clear" and "probably clear" within the footprint. The detailed cloud information for each AIRS FOV is then used to perform cloud-clearing for those partly cloudy IFOVS. Both "clear" and "overcast" pixels are left alone without any further processing.

2.3 Review of multiband cloud clearing approach

Traditional cloud clearing approach uses a single IR window spectral band. Smith et al. (2004) used the MODIS IR window spectral band (band 31, 11 μm) clear radiance together with the AIRS cloudy radiances convolved with MODIS 11 μm spectral response function (SRF) within two adjacent footprints to determine cloud-clearing parameter, N^*,

$$N^* = \frac{f_{31}(R_\nu^1) - R_{M_{31}}^{clr}}{f_{31}(R_\nu^2) - R_{M_{31}}^{clr}}, \tag{1}$$

where f_{31} is the MODIS IR band 31 spectral response function (SRF), and $R_{M_i}^{clr}$ is the mean of collocated observed clear radiances of MODIS IR spectral band 31 within two adjacent AIRS footprints, 1 and 2. Subscript 31 is MODIS band number, superscript 1 and 2 are for IFOV index, superscript clr denotes clear, and subscript M denotes mean value. The cloud-clearing parameter N^* can be explained as the extrapolation factor to derive clear radiances from two distinct cloudy radiances, assuming the same cloud type is observed in two AIRS footprints, a reasonable assumption for neighboring pixel measurements. Once N^* is determined by Eq. (1), the AIRS cloud-cleared spectrum R_ν^{cc} can be determined by the following equation:

$$R_\nu^{cc} = \frac{R_\nu^1 - R_\nu^2 N^*}{1 - N^*}, \tag{2}$$

where R_ν^1 and R_ν^2 are two AIRS cloudy radiance spectra (radiances as a function of wavenumber ν) corresponding to two adjacent IFOVs (IFOV 1 is the principal, while IFOV 2 is the supplementary).

The N^* value determined from a single MODIS spectral band, when using different MODIS IR window spectral bands, may result in a different cloud-cleared parameter and thus different cloud-cleared spectra. Uncertainty in N^* caused by observation error (radiance measurement error due to random senor noise, calibration uncertainty, and other abnormalities) can be difficult to detect, nevermind correct.

To improve the single channel cloud-clearing performance, an optimal N^* parameter to achieve reliable cloud-clearing using multiband cloud-clearing methodology is developed (Li et al., 2005b). The multiband N^* in Eq. (3) is determined not only by minimizing the differences between one single MODIS IR channel but also from other cloud sensitive window channels.

Similar to radiance observations and the convoluted AIRS CCR spectrum with SRFs for all nine MODIS IR spectral bands (band 22, 24, 25, 28, and 30–34) within IFOV 1 (the principal IFOV), the MODIS bands are weighted in the N^* calculation.

$$N^* = \frac{\sum_i \frac{1}{\sigma_i^2}[f_i(R_\nu^1) - R_{M_i}^{clr}][f_i(R_\nu^1) - f_i(R_\nu^2)]}{\sum_i \frac{1}{\sigma_i^2}[f_i(R_\nu^2) - R_{M_i}^{clr}][f_i(R_\nu^1) - f_i(R_\nu^2)]}, \quad (3)$$

where σ_i is the radiance detector noise (NEdR) for MODIS band i, and f_i is the MODIS SRF for band i. Once N^* is determined by Eq. (3), the cloud-cleared AIRS radiance spectrum can be retrieved by applying N^* to Eq. (2).

Note that each cloud sensitive MODIS channel is normalized to its expected measurement noise level in order to optimize its individual contribution in the deriving N^*. This multichannel cloud-clearing approach has been shown to achieve reliable results and is adopted in this paper to conduct the following cloud-clearing analysis.

2.4 AIRS and MODIS synergistic cloud-clearing procedure

AIRS spatial distribution is used in the collocation between the AIRS and MODIS measurements; this is the first step for the multiband MODIS/AIRS cloud-clearing procedure.

Using MODIS 1-km cloud mask to identify the MODIS clear pixels within each AIRS IFOV, the AIRS IFOVs can then be classified as fully cloudy, partly cloudy, or clear. Only AIRS IFOVs classified as partly cloudy are used for cloud clearing. Figure 1 shows the diagram of the principle IFOV and its eight surrounding supplementary IFOVs in the multiband cloud-clearing procedure.

Using multiband MODIS/AIRS cloud-clearing algorithm, calculate $N^*(k)$ in Eq. (3) for each pair (l,k), ($k = 1, 2, \ldots, 8$), then calculate $R_\nu^{cc}(k)$ ($k = 1, 2, \ldots, 8$) from Eq. (2), calculate minimum radiance and apply colocated MODIS clear radiances to derive cloud-cleared radiances and to perform quality control to choose the final CCR radiance spectrum. Nearby AIRS clear radiances are used to verify algorithm performance and to account for the scene inhomogeneity (will be discussed in Section 3.2.1). Estimation of cloud-clearing error is also included by way of granule-based RMS difference and Bias spectra separately for day, night, and over land and ocean areas.

In summary, MODIS/AIRS cloud clearing procedure can be further summarized as follows:

1) Colocate all MODIS pixels falling within AIRS IFOV.

2) Using MODIS 1 km cloud mask to identify the MODIS clear pixels within each AIRS IFOV. The mean of these clear radiances is prepared as $R_{M_i}^{clr}$ for N^* derivation.

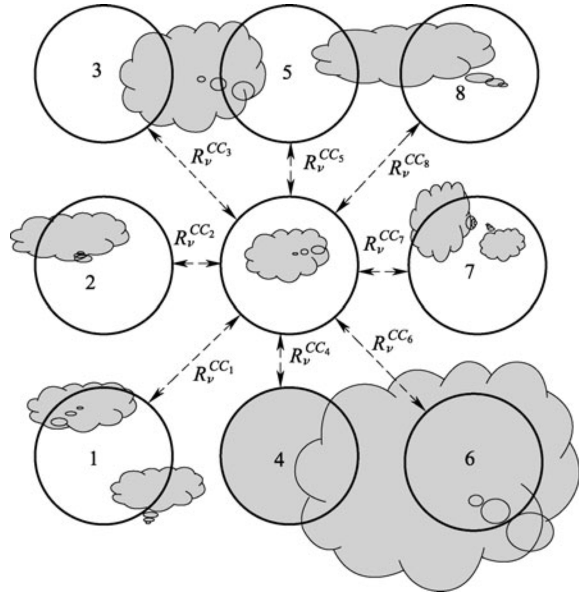

Fig. 1 Diagram of the principle IFOV and its eight surrounding supplementary IFOVs in the multiband cloud-clearing procedure

3) Using multichannel N^* algorithm Eq. (3) to estimate N^*.

4) Use Eq. (2) to retrieve cloud-cleared radiances, R_ν^{cc}.

5) Using colocated MODIS clear radiances (not used for the derivation of N^*) to perform quality control. For those differences between cloud-cleared and colocated clear radiances that are greater than their specific noise level, the cloud-cleared flag is to be set to unsatisfactory.

6) Using nearby AIRS clear radiances to verify the derived AIRS cloud-cleared performance and to account for the scene inhomogeneity effect.

7) Estimate cloud-clearing error by way of granule-based Root Mean Square Difference (RMSD) and Bias spectra independently for day, night, and over land and over water surfaces.

3 Global AIRS/MODIS cloud clearing

3.1 AIRS global cloud clearing

It has been demonstrated that for any satellite infrared sounder with a relatively wide field of view (IFOV > 10 km), the probability of entirely cloud-free observation is surprisingly low. Figure 2 shows the frequency of AIRS clear FOV for all granules on January 1, 2004, and the global average is about 5% to 15% for AIRS FOV to be confident clear.

Using multiband cloud clearing method, the synergistic MODIS and AIRS cloud clearing is applied to all AIRS

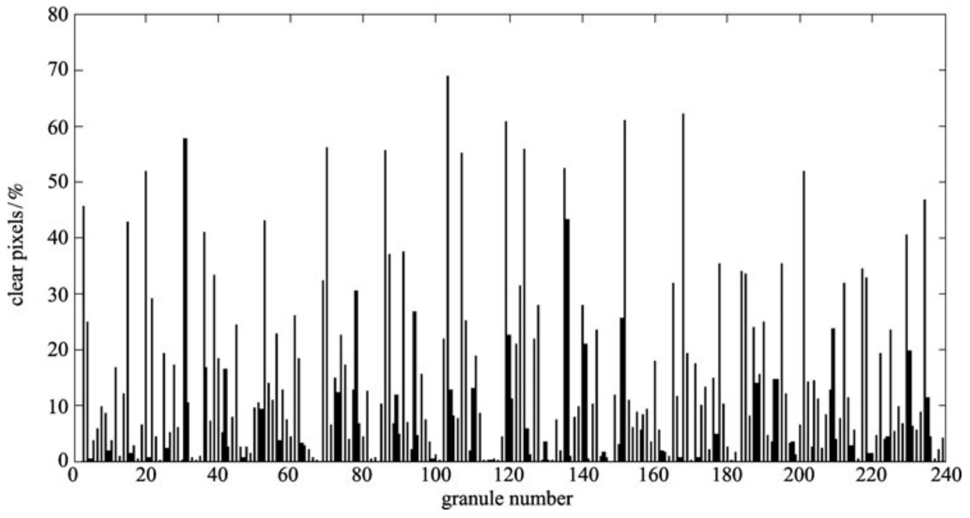

Fig. 2 AIRS global clear FOV frequency on January 1, 2004

IFOVs that are partly cloudy only. For those either confident clear or fully cloudy (overcast) IFOVS, no cloud-clearing is performed. The confident clear AIRS IFOVS are used as independently clear radiances for the estimation of the error of cloud-cleared radiances (to be discussed in the later section). There are four categories in the AIRS cloud clearing FOVs: clear, cloud-clearing successful (CCS), cloud-clearing failed (CCF), and fully cloudy.

3.1.1 Daily analysis

Figure 3 is an example of AIRS cloud clearing on July 15, 2007. It depicts the following:

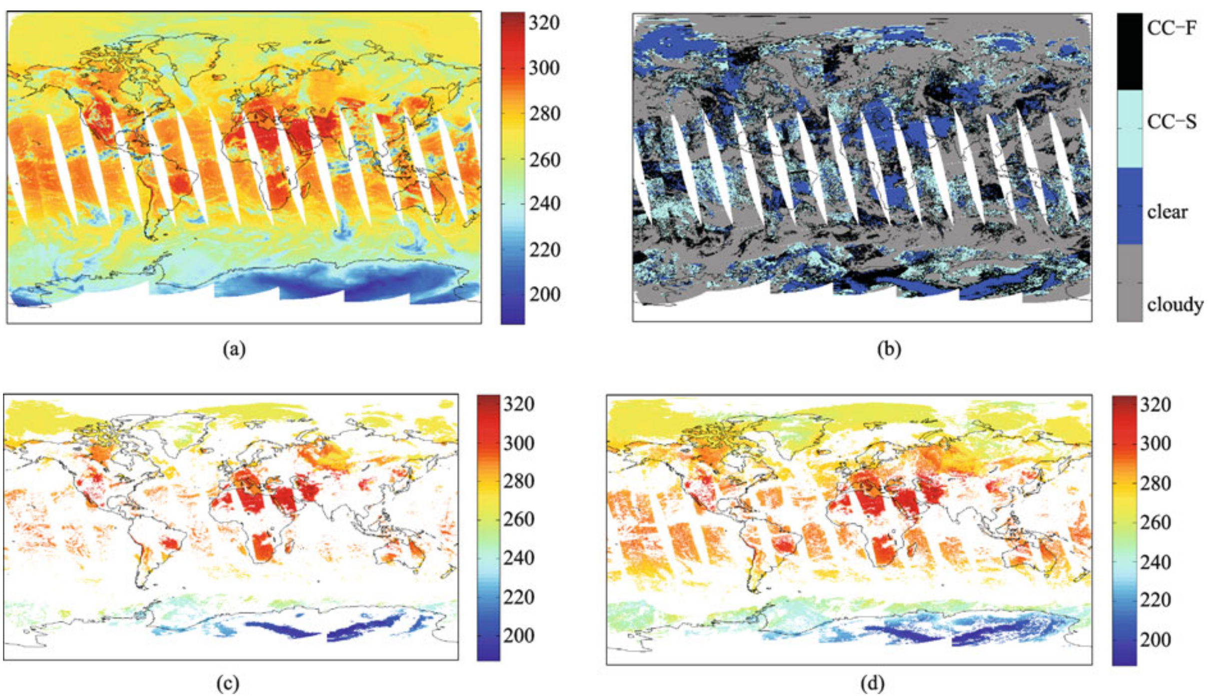

Fig. 3 (a) One day global FOV brightness temperature (BT) day time at AIRS wavenumber 1000 cm^{-1} on July 15, 2007; (b) the AIRS cloud-clearing flag of (a), the color bar (vertical bar in the right hand side) represents cloud clearing fail (CCF), cloud clearing successful (CCS), clear, and cloudy; (c) global clear only FOV brightness temperature (BT) of (a); (d) global clear and cloud clearing successful FOVs

(a) It is one full daytime day of brightness temperature (BT) of AIRS wavenumber 1000 cm^{-1}.

(b) It is the AIRS cloud clearing flag image, where the color bar (the right vertical bar) represents flag of cloud clearing failed (CCF) in black, cloud clearing successful (CCS) in cyan, clear in blue, and fully cloudy in gray.

(c) It is globally clear, only IARS IFOV brightness temperature (BT) image shown for reference.

(d) It shows both clear and cloud clearing successful FOVs. The increased coverage when compared to Fig. 3 (c) illustrates the yield increases due to successful cloud clearing.

Two days of cloud clearing statistics are shown for comparison. For January 1 and September 1, 2007, the two days' percentages of successful synergistic cloud clearing are similar: 11.54% vs. 13.91%. Figure 4 shows that there are about 12% CC-S for January 1 (Fig. 4(a)) and 13% CC-S for September 1 (Fig. 4(b)), 2007, which make a total clear FOV about 25% instead of 13% clear FOV globally, i.e., almost double.

3.1.2 Monthly analysis

Figure 5 presents daily details of AIRS cloud-clearing processing performance for January (Fig. 5 (a)) and August (Fig. 5 (b)) in 2007. The results show the consistency for each day. On the average, globally, it is about 13% clear, 7% CCS during day time, 5% CCS at night, 30% CC failed, and 45% fully cloudy. After synergistic cloud clearing, there are almost doubled clear IFOVs, and CCS at day time is about 2% more than night time due to the fact that MODIS cloud mask takes advantage of visible measurement information, being more accurate during day time. The consistent results indicate that the synergistic cloud-clearing is robust, and its performance depends somewhat upon MODIS cloud mask.

3.1.3 Seasonal analysis

Seasonal AIRS CC global statistics are shown in Fig. 6. Figure 6 (a) shows the performance from winter season

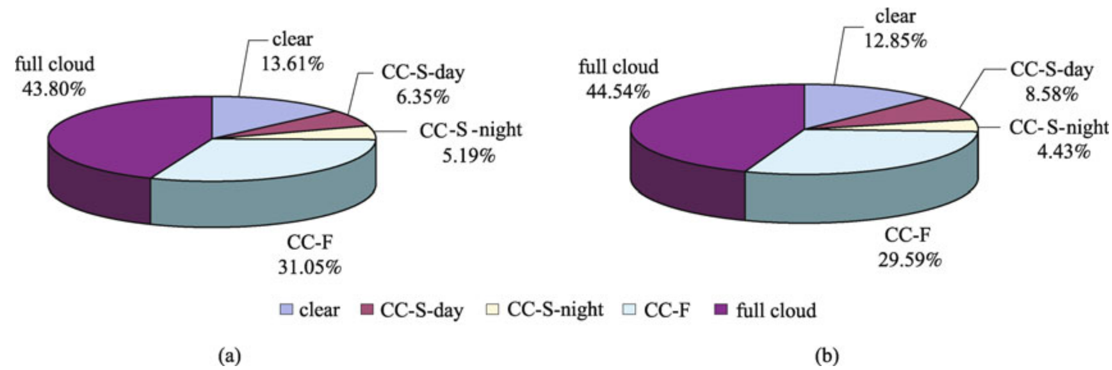

Fig. 4 AIRS global cloud clearing statistics on January 1st (a) and September 1st (b) 2007

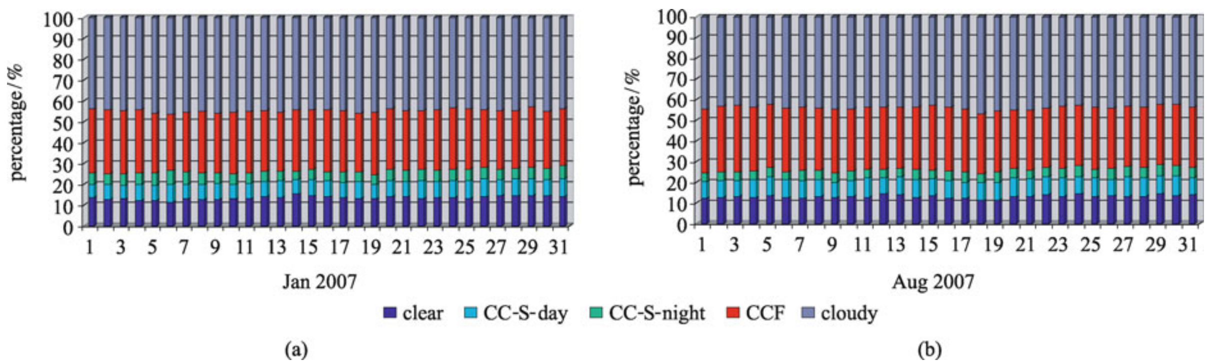

Fig. 5 Global AIRS cloud clearing IFOV processing statistics for January (a) and August (b) in 2007

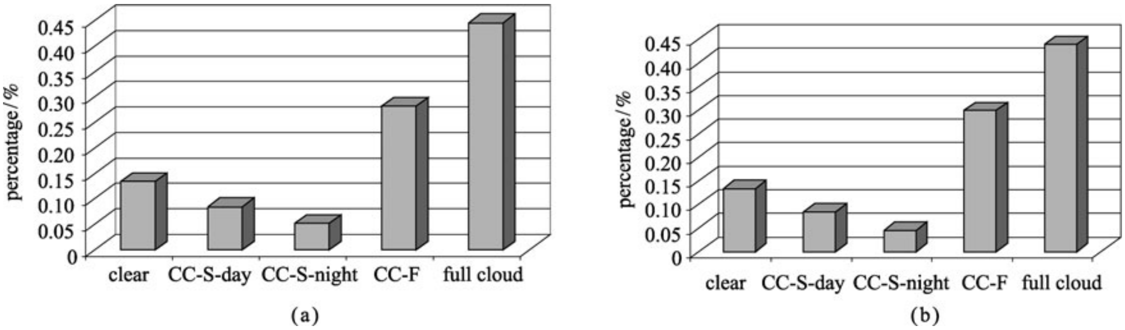

Fig. 6 Seasonal AIRS CC global statistics, winter season (Jan., Feb., and Mar.) (a) and summer season (Jul., Aug., and Sep.) (b) in 2007

(January, February, and March). Figure 6 (b) shows the same statistics in Fig. 6 (a) but for summer season (July, August, and September). The results from both seasons are consistent. Again, the seasonal average is similar to monthly or daily means where the successful cloud clearing is similar to the percentage of the confident clear pixels. No significant difference exists between winter and summer season and also daytime performs better than night time due to the quality of MODIS cloud mask that guides this synergistic cloud-clearing process.

3.2 Bias and RMS error of cloud cleared vs. nearby clear

3.2.1 Daily bias analysis

For IFOVs deemed successfully cloud cleared, the cloud-cleared radiances need to be analyzed to ensure that cloud contamination has indeed been removed. To evaluate the performance of AIRS cloud-clearing radiances, the bias, standard deviation, and the root mean square difference (RMSD) were studied, daily, monthly, and seasonally. Figure 7 (a) shows the bias between the AIRS cloud-cleared spectra and their nearby clear IFOV spectra over land (upper panel) and ocean (lower panel) on January 1, 2007. It is assumed that the nearby (within 3 by 3 AIRS IFOV area) confident clear is the “true clear” that can be used to assess the accuracy of the cloud-cleared spectra. Note that the error introduced by the scene inhomogeneity that makes this assumption imperfect and will be dealt with in the following section. Without accounting for the scene inhomogeneity, it can be seen that the bias is less than 0.2 over land and less than 0.1 over ocean for the spectral region of 600 to 2400 cm^{-1}. A slightly larger bias exists between the 2400 to 2600 cm^{-1} region. Overall, there is smaller bias over ocean than over land because the land surface variation is usually much larger than the ocean. The root mean square difference (RMSD) of AIRS cloud-cleared BTs is less than 2 K for most spectral regions in Fig. 7 (b). The assumption of using the nearby clear as the “truth” for validating the cloud-cleared error suffers the from the inherent scene inhomogeneous effect. The scene inhomogeneous effect was studied for both over land (Fig. 7 (b)) and over ocean (Fig. 7 (c)). RMSD with the scene inhomogeneous correction is about 1K less than the RMSD without the scene inhomogeneous correction over land and 0.5K less over ocean.

Inhomogeneity features, especially land inhomogeneity issues, affect the error estimation. Scene InHomogeneity Estimation (SI-HE) C_{SI} relies on statistics calculated locally by Eq. (4):

$$C_{SI} = \frac{1}{N}\sum_{i} \mathrm{abs}([(R_i^{clr} - R_j^{clr}])/D_{i,j}, \quad (4)$$

where j is the near by clear IFOV of I ; $D_{i,j}$ is the distance between clear IFOV i and clear IFOV j.

Corrected CC radiance R_{corr}^{cc} after SI-HE is calculated by Eq. (5)

$$R_{corr}^{cc} = R^{cc} - C_{SI}*D_{cc,clr}, \quad (5)$$

$D_{cc,clr}$ is the distance between CC IFOV and nearby clear IFOV.

3.2.2 Monthly bias analysis

Systematic error (i.e., bias) for each month was studied. Figure 8 shows the bias analysis in January as follows: (a) It shows the monthly bias between the AIRS CCS BT spectra and their nearby clear IFOV BT spectra over land (upper panel) and ocean (lower panel) surface in Jan. 2007. This comparison includes the effect of scene inhomogeneity as depicted by the plots that the bias is larger over land than ocean surface. (b) it is the monthly bias between the AIRS convolved CCS BT and the collocated MODIS clear measurements at MODIS bands in Jan. 2007 for day and night time over land and ocean surface, respectively. The CC bias for MODIS bands 22–24, and 30 through 36 are very small (less than 1 K). However, bias for bands 20, 27–29 are relatively large due to the convolution bias (Tobin et al., 2004). The AIRS popping channels and the AIRS spectral gap cause the convolution bias. MODIS

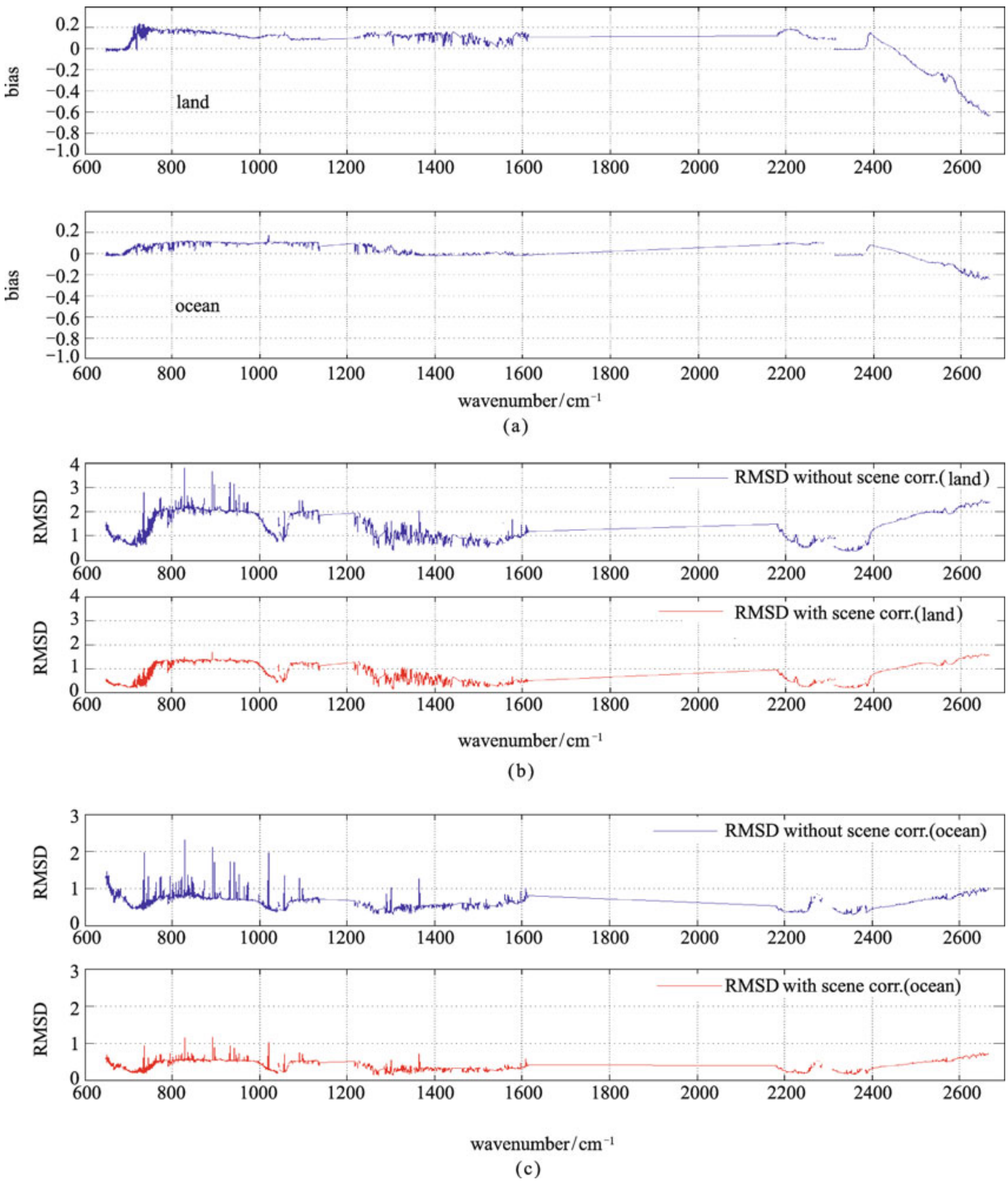

Fig. 7 Global AIRS cloud clearing statistics on Jan. 1, 2007. (a) Bias for land surface (upper panel) and ocean surface (lower panel) between the AIRS cloud-cleared BT spectra and their nearby clear footprint BT spectra; (b) the same as (a) but for RMSD with/without Scene In-Homogeneity Correction over land surface; (c) the same as (b) but for RMSD over ocean surface

bands 35 and 36 might also have an SRF calibration bias. The performance is consistent at day and nighttime when MODIS cloud mask characteristic is taken into account. This comparison is relatively close to the best possible estimate of the synergistic MODIS/AIRS cloud clearing performance since the collocated clear radiances within the AIRS IFOV represent the best estimate of the clear radiance measurements for those MODIS channel that are not used in the cloud clearing. (c) It shows the comparison of monthly RMSD between the AIRS CCS BT spectra and their nearby clear footprint BT spectra over land with and without Scene InHomogeneity correction (SIH) in Jan. 2007. SIH reduces the CC errors due to the correction of scene inhomogeneous effect. (d) It is the same as (c) but over ocean surface. Oceanic surface properties are roughly constant over an AIRS IFOV. RMSD over the ocean is smaller than over land, because the ocean surface due to less complicated ocean surface feature has higher quality cloud mask, and a smaller degree of scene inhomogeneity that needs to be corrected.

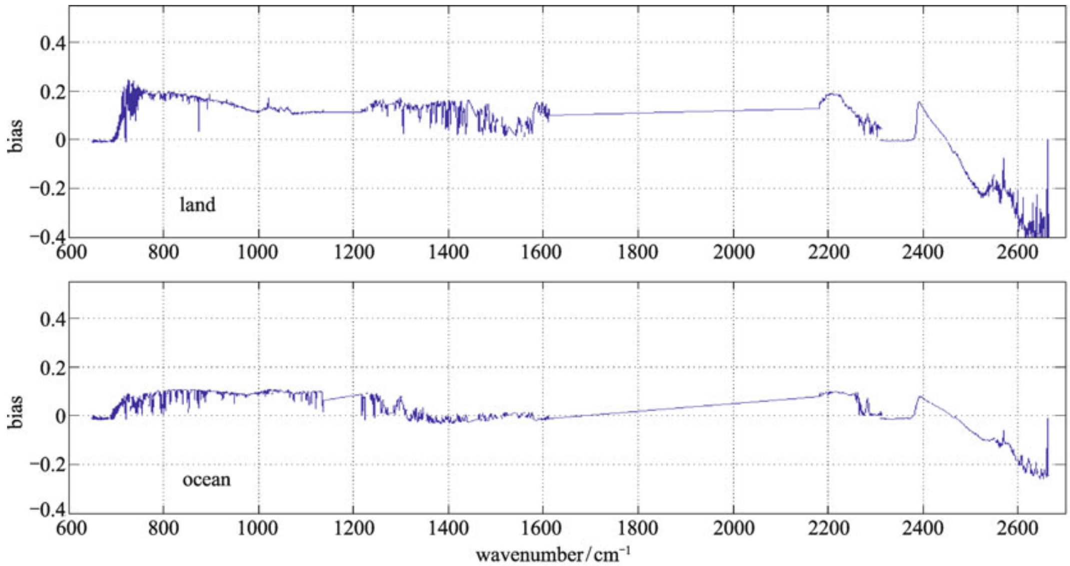
bias
land
ocean
wavenumber/cm⁻¹

(a)

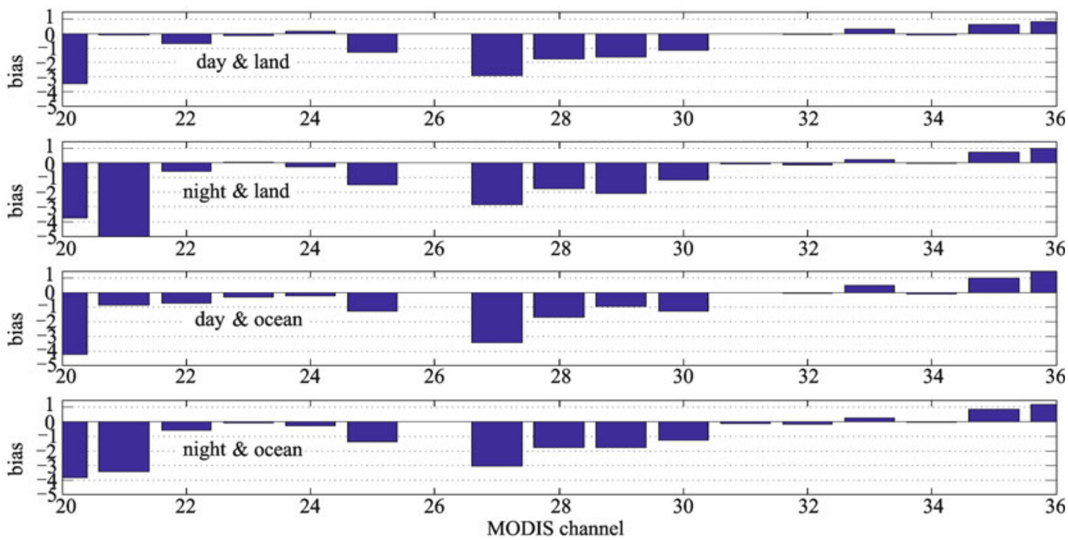
bias
day & land
night & land
day & ocean
night & ocean
MODIS channel

(b)

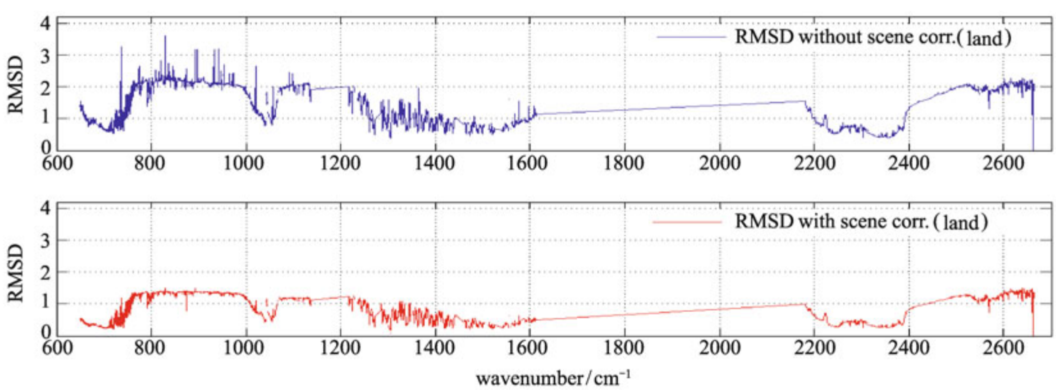
RMSD
RMSD without scene corr.(land)
RMSD with scene corr.(land)
wavenumber/cm⁻¹

(c)

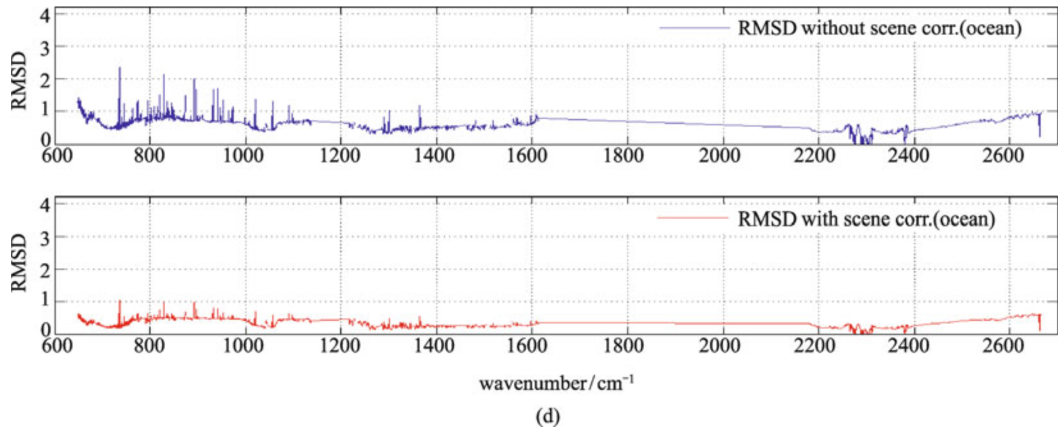

Fig. 8 Monthly bias in Jan. 2007 between the AIRS CCS BT spectra and their nearby clear footprint BT spectra; (a) the monthly bias over land (upper panel) and ocean (lower panel) surface; (b) the monthly bias between the AIRS convolved CCS BT and the collocated MODIS clear measurements at MODIS bands for day and night time over land and ocean surface, respectively; (c) the comparison of monthly RMSD over land with and without SIH correction; (d) the same as (c) but over ocean surface

3.2.3 Seasonal bias analysis

Seasonal AIRS CC global statistics have been analyzed. In this paper, we define the season of January, February, and March as winter and the season of July, August, and September as summer. Figure 9 (a) shows the statistics from winter season, during which there are 13.42% clear pixels, 8.49% CC-S during daytime and 5.21% at night, resulting in a total of 27.12% clear pixels. That is nearly double the clear pixels from the summer season. Figure 9(b) shows the very similar results for summer. During summer, there are 13.35% clear pixels, 8.38% cloud clear successful during day time, and 4.47% CCS at night. Both summer and winter statistics are very consistent, which indicate that the cloud clearing algorithm produces consistent results throughout the year.

Figure 10 shows the seasonal bias between the global AIRS CCS BT spectra and their nearby clear IFOV BT spectra over land (Fig. 10(a)) and ocean (Fig. 10(b)) for both winter (blue) and summer (red). Bias over land during winter is smaller than in summer. However, there is not much difference over ocean between winter and summer. Results over the land surface also show that summer has more variance than winter.

Seasonal global RMSD were studied between the AIRS CCS BT spectra and their nearby clear footprint BT spectra. Figure 11 presents the global RMSD over land during winter season (Fig.11 (a)) and summer season (Fig.11 (b)). RMSD over the ocean surface is not shown here because the ocean surface is smooth, and its RMSD is much less than the RMSD over land. RMSD without Scene InHomogeneity correction (SIH) were shown in the upper panels. The middle panels show the RMSD with SIH correction. The lower panels show the comparison

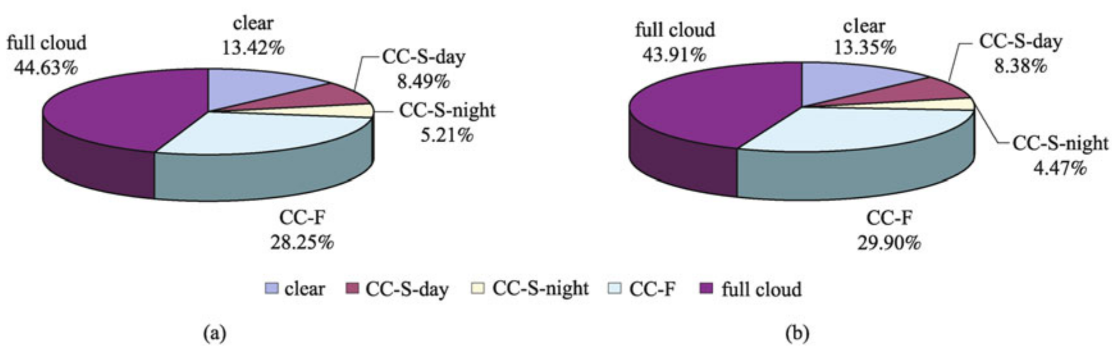

Fig. 9 Seasonal AIRS CC global statistics: summer season (Jan., Feb., and Mar.) (a) and winter season (Jul., Aug., and Sept.) (b)

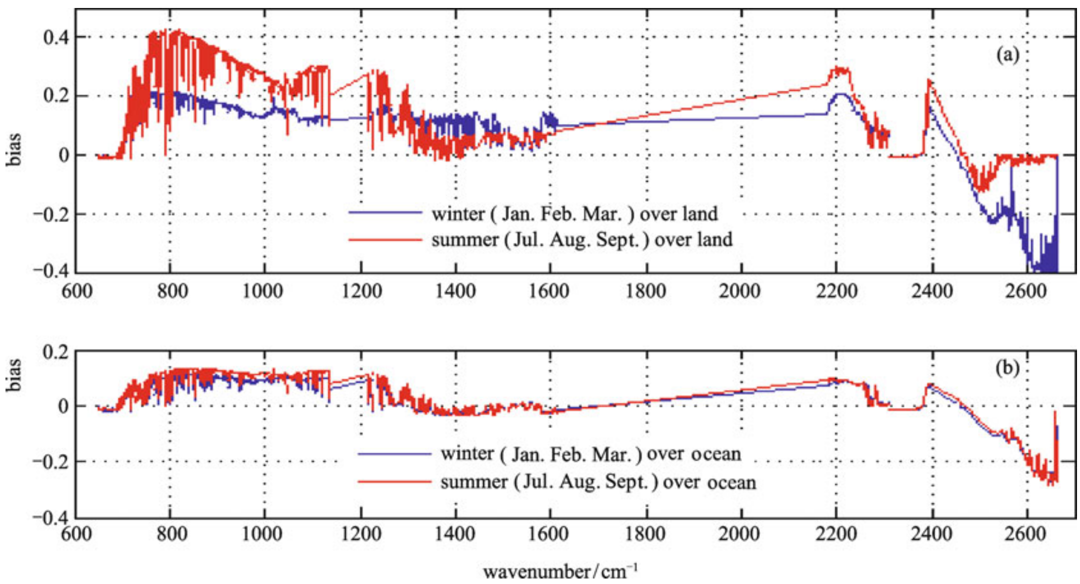

Fig. 10 Seasonal bias of AIRS CC global statistics in 2007. (a) Land; (b) ocean

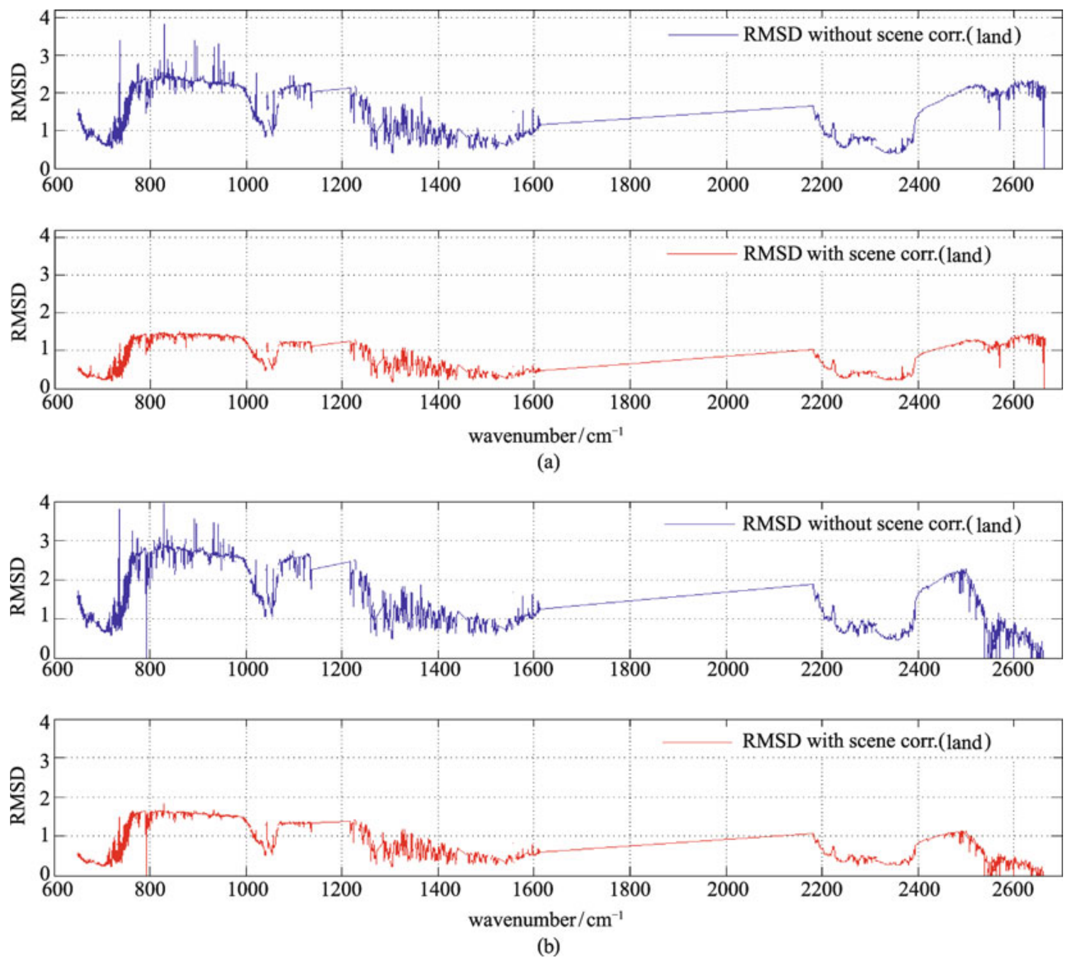

Fig. 11 Seasonal global RMSD between the AIRS CCS BT spectra and their nearby clear footprint BT spectra over land during winter (Jan., Feb., and Mar.) (a) and summer (Jul., Aug., and Sept.) season (b) in 2007

between with/without SIH correction. The SIH correction yields consistent seasonal variation.

4 Conclusions

One year of collocated AIRS/MODIS global data for the year 2007 has been generated. The performance of MODIS/AIRS synergistic cloud cleared radiances in daily, monthly, and seasonal analysis are consistent for both land and water surfaces when IFOV to IFOV scene variation is taken into account. The results have shown that, globally, about 13% of AIRS partial cloudy IFOVs can be successfully cloud cleared. Cloud-cleared and clear AIRS observations double the percentage of 'cleared' IFOVs from 13% to about 26%. The synergistic AIRS/MODIS cloud-clearing performance in terms of bias and RMSD error using collocated MODIS clear and nearby AIRS clear data has been studied. The cloud-cleared radiances dataset along with their associated error estimates are helpful for potential assimilation of AIRS cloud-clearing radiances. In addition, the MODIS/AIRS synergistic cloud-clearing and retrieval using cloud-cleared AIRS radiances will be packaged into MODIS/AIRS Processing Package (IMAPP) (Huang et al., 2004) for future release. Synergistic imaging and sounding cloud-clearing approach will also be adopted for the future geostationary cloud-clearing processing, where high spatial resolution imaging and hyperspectral sounding data are available to improve the yield of the clear sounding probability.

Our future work will include the use of integrated infrared imaging and sound and microwave data, such as MOIDS, AIRS, and AMSU, to optimize the retrieval performance under various cloudy conditions, especially for those nearly 30% of failed MODIS/AIRS cloud-clearing cases. Continued refinement of MODIS/AIRS synergistic cloud-clearing and their objective estimation of the cloud-clearing induced error will also be a focus.

References

Ackerman S A, Strabala K I, Menzel W P, Frey R A, Moeller C C, Gumley L E (1998). Discriminating clear sky from clouds with MODIS. J Geophys. Research-Atmospheres, 103 (D24): 32141–32157

Aumann H H, Chahine M T, Gautier C, Goldberg M D, Kalnay E, McMillin L M, Revercomb H, Rosenkranz P W, Smith W L, Staelin D H, Strow L L, Susskind J (2003). AIRS/AMSU/HSB on the Aqua mission: design, science objectives, data products, and processing systems. IEEE Trans Geosci Rem Sens, 41 (2): 253–264

Huang H L, Gumley L E, Strabala K, Li J, Weisz E, Rink T, Baggett K C, Davies J E, Smith W L, Dodge J C (2004). International MODIS and AIRS Processing Package (IMAPP): A direct broadcast software for the NASA earth Observing System. Bull Am Meteorol Soc, 85 (2): 159–161

Huang H L, Smith W L (2004). Apperception of clouds in AIRS data. In: Proceeding ECMWF Workshop on Assimilation of High Spectral Resolution Sounder in NWP, June 28–July 1, 2004, 155–169

Li J, Huang H L, Liu C Y, Weisz E, Guan Li, Yang P, Wei H L, Schmit T J, Menzel W P (2005a). Retrieval of cloud microphysical properties from MODIS and AIRS. J Appl Meteorol, 44 (10): 1526–1543

Li J, Liu C Y, Huang H L, Schmit T J, Wu X B, Menzel W P, Gurka J J (2005b). Optimal cloud-clearing for AIRS radiances using MODIS. IEEE Trans Geosci Rem Sens, 43 (6): 1266–1278

Li J, Menzel W P, Sun F, Schmit T J, Gurka J (2004). AIRS sub-pixel cloud characterization using MODIS cloud products. J Appl Meteorol, 43 (8): 1083–1109

Smith W L, Zhou D K, Huang H L, Li J, Liu X, Larar A M (2004). Extraction of profile information from cloud contaminated radiances. In: Proceeding ECMWF Workshop on Assimilation of High Spectral Resolution Sounder in NWP, June 28–July 1, 2004, 145–154

Tobin D C, Revercomb H E, Moller C C, Knuteson R O, Best F A, Smith W L, van Delst P, LaPorte D D, Ellington S D, Werner M D (2004). Validation of Atmospheric InfraRed Sounder (AIRS) spectral radiances with the S-HIS aircraft instrument. In: Remote Sensing of Cloud and the Atmosphere IX, Proceedings of SPIE 5571, 13–15 Sepetember 2004, Maspalomas, Gran Canaria, Spain

Zhang Z B, Yang P, Kattawar G, Huang H L, Greenwald T, Li J, Baum B, Zhou D K, Hu Y (2006). A Fast Infrared Radiative Transfer Model Based on the Adding-Doubling Method for Hyperspectral Remote Sensing Applications. J Quantitative Spectroscopy & Radiative Transfer (in press)

Zhang H, Huang H L, Li J, Weisz E, Baggett K, Liu C Y (2007). Global Analysis and Characterization of AIRS/MODIS Cloud-Clearing. In: IUGG, July 2–13, 2007, Perugia, Italy